Canadian Chemical Transactions
ISSN 2291-6458 (Print), ISSN 2291-6466 (Online)
Year 2013 | Volume 1 | Issue 2 | Page 85-104

Review

DOI:10.13179/canchemtrans.2013.01.02.0021

Clinical Diagnosis of Bacterial Infection via FDG-PET Imaging

Zhirui Wang[1]* and Xinghai Ning[2]*

[1]*Complex Carbohydrate Research Center, University of Georgia, Athens, GA 30602, USA*
[2]*Department of Bioengineering, UC Berkeley, Berkeley, CA 94720, USA*

**Corresponding Author, Email: wangzr@uga.edu xning8@berkeley.edu Phone: +1-706-248-7035 (Z. W.) and +1-706-248-4936 (X. N)*

Received: *May 7, 2013* ***Revised:*** *May 19, 2013* ***Accepted:*** *May 19, 2013* ***Published:*** *May19, 2013*

Abstract: The key challenge in the treatment of bacterial infection is rapid identification of bacteremia at an early stage of the diseases. Currently available imaging systems such as computed tomography (CT) and magnetic resonance imaging (MRI) can only detect bacterial infection after they have become systemic or have caused significant anatomical tissue damage, and at this stage infection are challenging to treat due to the high bacterial burden. To this day positron emission tomography (PET) imaging has showed the great potential for improving the diagnosis of bacterial infection because of the high sensitivity of PET radionuclides, capability of detecting molecular biology in details (even prior to anatomic change). Fluorodeoxyglucose (FDG) PET has been developed for bacterial imaging with incredible success. Whole body PET imaging with FDG for the diagnosis of bacterial infection and monitoring response to treatment has been well established. FDG-PET will not only help to accelerate the diagnosis of infection but improve the bacterial treatment. In this review, we focus on FDG-PET imaging for diagnosing bacterial infection in the clinic.

Keywords: Fluorodeoxyglucose, Positron Emission Tomography, Bacterial Infection, Molecular Imaging

1. INTRODUCTION

Bacterial infection is one of the leading causes of death and causes millions of people dead every year in the world [1-5]. Owing to its multiple routes of transmission, early diagnosis is critical to the prevention and treatment of bacterial infection. Traditional identification methods for the infection focus on the examination and culture of bacteria recovered from suspicious sites [6-8]. Despite these methods

ISSN 2291-6458 (Print), ISSN 2291-6466 (Online)
Year 2013 | Volume 1 | Issue 2 | Page 85-104

are powerful and error-proof, they are laborious, complex and time-consuming, and the results are often obtained too late to guide clinical decision making. Detection and localization of infectious foci in soft tissues can also be achieved by ultrasound, CT or MRI, which is effective in detecting inflammation whenever the lesion has caused changes in local anatomy, capillary permeability, or tissue water content [9,10]. However, when normal anatomic landmarks are lost or obscured, infection cannot be identified, and, in particular, it is difficult or impossible to distinguish between bacterial infection and sterile inflammation by these means. Therefore, there is the great need of developing new methods to diagnose bacterial infection with high sensitivity and specificity.

Nuclear imaging technology, which produces a three-dimensional image or picture of functional processes in the body, has great potential to improve the diagnosis of bacterial infection due to its high sensitivity to radionuclides, capability of detecting molecular biology in details and widespread clinical use [7,8,11-13]. However, it cannot provide precise signal localization of infection due to its low spatial resolution and the lack of anatomical information. To overcome its limitation, the new fused imaging technologies, such as PET/CT and PET/MRI, have been developed with the ability to provide a simultaneous atomical and physiological assessment, allowing PET imaging more and more popular for the clinical diagnosis [13-18]. Numerous radiopharmaceuticals have been available for imaging bacteria, such as radiolabeled antibiotics, antibodies, antimicrobial, chemotactic peptides, bacteriophages and leukocytes (see in table 1), but most of them has limited application [6-8,11,12].

The radiotracer FDG is the most widely used radionuclide and can be used for the assessment of glucose metabolism in the most organs. Although most FDG research focuses imaging tumors in oncology, it is also a powerful diagnostic tool in imaging infectious diseases or other inflammatory disorders [14-18]. In this article, we report the benefit and diagnostic value of FDG-PET in the assessment of bacterial infection.

Table 1. Currently reported nuclear medicine techniques for bacterial detection

Approved Radiopharmaceuticals	Investigational Radiopharmaceuticals
^{67}Ga citrate	^{111}In-DTPA-human IgG (HIG)
^{111}In- oxine to labele leucocytes in vitro	^{99m}Tc-HYNIC-IgG (HIG)
^{99m}Tc-HMPAO to labele leucocytes in vitro	^{99m}Tc-anti-NCA-95 IgG
^{99m}Tc-anti-NCA granulocyte antibody	^{111}In-F(ab)$_2$-anti-E-selectin antibody
^{99m}Tc-anti-SSEA-1 IgM to labele leucocytes in vivo	^{99m}Tc-Interleukin-8 (IL-8)
^{99m}Tc-ciprofloxacin	^{99m}Tc labeled chemotactic peptides leucocytes
^{18}F-FDG	^{99m}Tc labeled nanocolloids
	^{18}F-FDG
	^{18}F-FDG-leukocytes (labeled in vitro)

2. FDG IMAGING

FDG is an analog of glucose in which the hydroxyl group on the 2-carbon of a glucose molecule is replaced by a fluoride atom. FDG can be synthesized by either electrophilic fluorination of 3,4,6-triacetyl-d-glucal (TAG) using acetylhypofluorite [19-21] or nucleophilic substitution of 1,3,4,6-tetracetyl-2-trifluoromethan sulfonyl-β-d-mannose [22-24] using potassium fluoride (shown in Figure 1).

ISSN 2291-6458 (Print), ISSN 2291-6466 (Online)
Year 2013 | Volume 1 | Issue 2 | Page 85-104

Due to the great radiochemical purity and especially higher specific activity available, coupled with the advantage of getting an epimeric pure product, the nucleophilic fluoration method is now the most common way to synthesize FDG. A series of automated synthesis modules have been reported to produce larger amounts of FDG in excellent radiochemical yield (about 70%) within an hour [22-25].

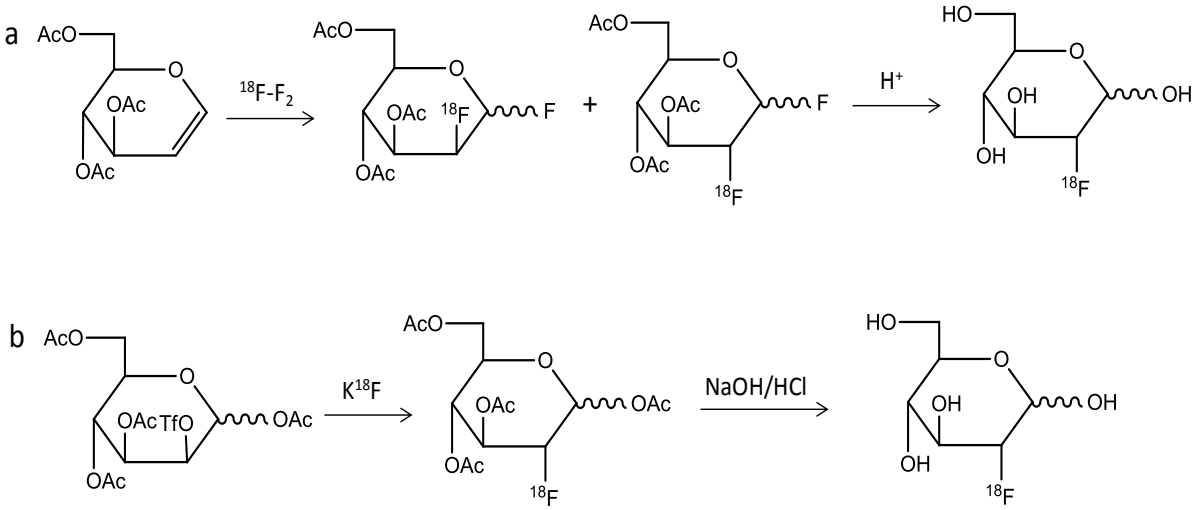

Figure 1. Synthesis of FDG by electrophilic (a) and nucleophilic substitution(b)

The accumulation of FDG in the targeted foci is based on enhanced glycolysis, which has often been associated with the cell growth rate and the expression of glucose transporters in cells. Like glucose that plays an essential role in the cellular energy metabolism, FDG is transported into cells via glucose transporters (mainly GLUT-1 and GLUT-3) and phosphorylated via hexokinase. Not like glucose, FDG cannot undertake further metabolism via G6-phosphate isomerase because of the absence of the 2-carbon hydroxyl group. Consequently, FDG-6-phosphate [21,26-29] is not able to be further degraded and will be trapped in the cell because of its negative charge (see detailed mechanism for FDG uptake in Figure 2). Therefore, FDG is able to monitor alterations in glucose metabolism, which is a marker for the viability of cells.

After intravenous administration, FDG routinely distributes to the major tissues [26,30,31] including brain, myocardium, and genitourinary tract, thymus, liver, spleen, bone marrow, and brown adipose tissue, and clears from urinary system (see Figure 3a). Tumor, inflamed or infected tissues internalize FDG more quickly than normal tissues [26,28,30-34], due to their overexpression of glucose transporters, enhanced glucose metabolism and increased tissue permeability (see Figure 3b). In order to reduce the uptake of FDG in normal tissues and increase the signal-to-noise ratio, patients and animals are normally fast for at least several hours prior to examination to reduce competition for glucose transporters. In addition, limitation of physical activity before injection can also minimize the tissue uptake of FDG, leading to low background [33,34]. Administration of benzodiazepines 30–60 minutes before FDG injection can also diminish activity in muscle and brown adipose tissue [35]. In the evaluation of the lower extremities, it is recommended to have the patient remain at bed rest for at least 1 hour prior to injection.

ISSN 2291-6458 (Print), ISSN 2291-6466 (Online)
Year 2013 | Volume 1 | Issue 2 | Page 85-104

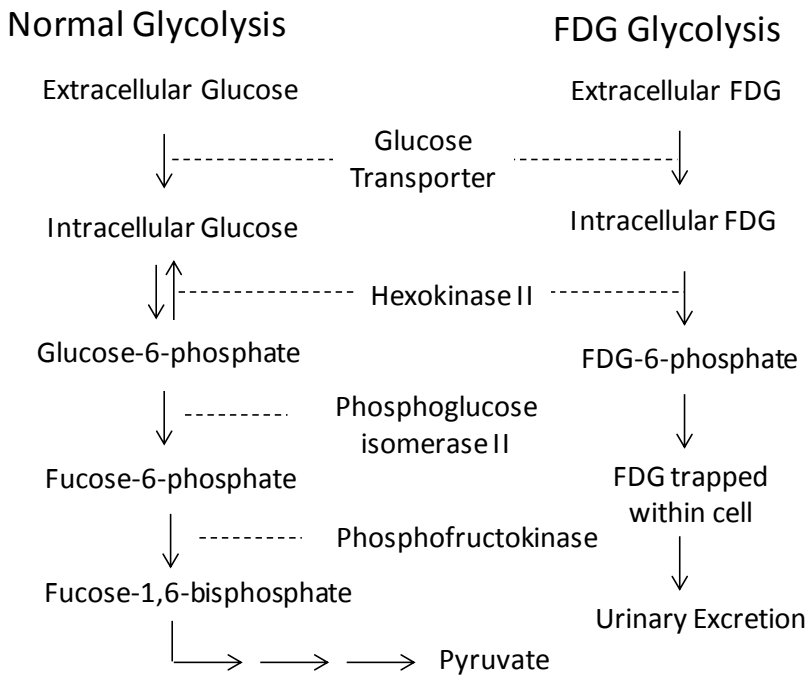

Figure 2. Schematic presentation of the FDG uptake mechanism: FDG is transported into the cell via glucose transporters (GLUT). In the cell FDG is phosphorylated via hexokinase-II. Introduction of the negative charge on the phosphate group is responsible for intracellular trapping. Due to the missing hydroxyl function at position 2′, FDG-phosphate is not tolerated by glucose-6-phosphate isomerase-II and cannot be metabolized.

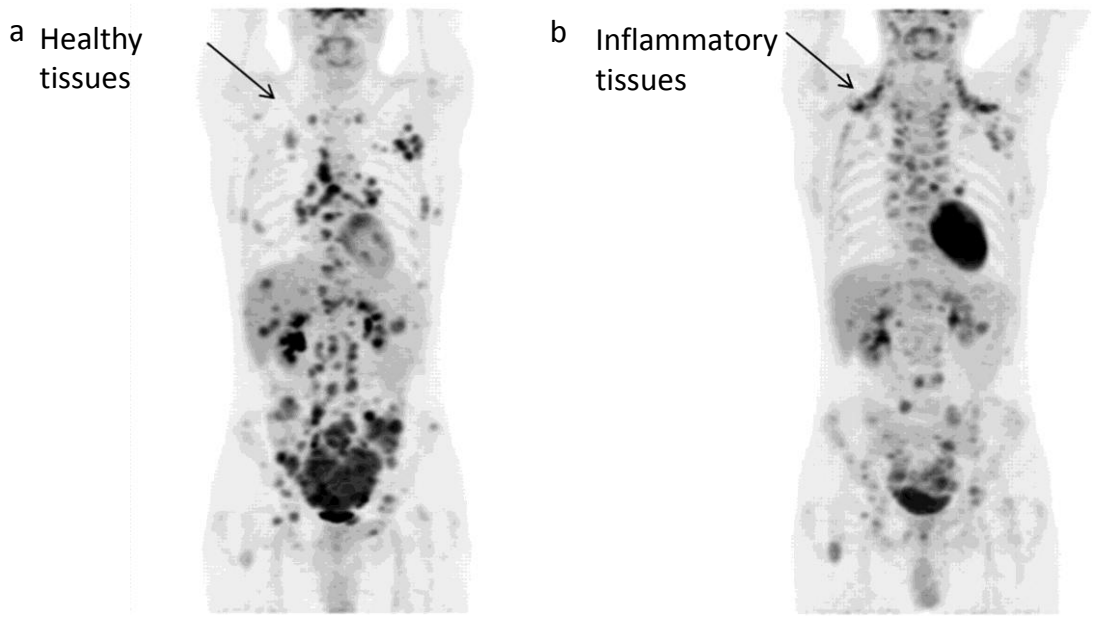

Figure 3. Whole-body Coronal PET images of a healthy human and a human with inflammatory disorders, Images reproduced with permission from [32], Copyright 2012, SNMMI.

ISSN 2291-6458 (Print), ISSN 2291-6466 (Online)
Year 2013 | Volume 1 | Issue 2 | Page 85-104

3. DIAGNOSIS OF DIFFERENT BACTERIAL INFECTION VIA FDG-PET IMAGING IN THE CLINIC

FDG-PET imaging has been widely used for diagnosing, staging, and detecting the recurrence or progression of cancer including breast, colorectal, esophageal, head and neck, lung, pancreatic, and thyroid cancer; lymphoma, melanoma, andsarcoma; and unknown primary tumor [12,14,26-28,30,32,33,36]. It has also been shown that FDG rapidly accumulates at the sites of bacterial infection with high target-background ratio compared with other tracers such as radiolabeled thymidine, L-methonine and iodine-125 human serum albumin [11,12,15-18,35]. FDG has been approved by US Food and Drug Administration (US FDA) and European Medicines Agency (EMEA) and authorized as a diagnostic radiopharmaceutical in the diagnosis of bacterial infection. However, this technique still lacks the solid support and evidence-based criteria even with the approval of its application for infection in the clinic. In some situations, it cannot yet be considered a sufficient replacement for labelled white blood cell (WBC) imaging or anti-granulocyte monoclonal antibody (MoAb) imaging [11]. In this article, we discuss and illustrate the role and limitations of FDG-PET in the assessment of bacterial infectious diseases.

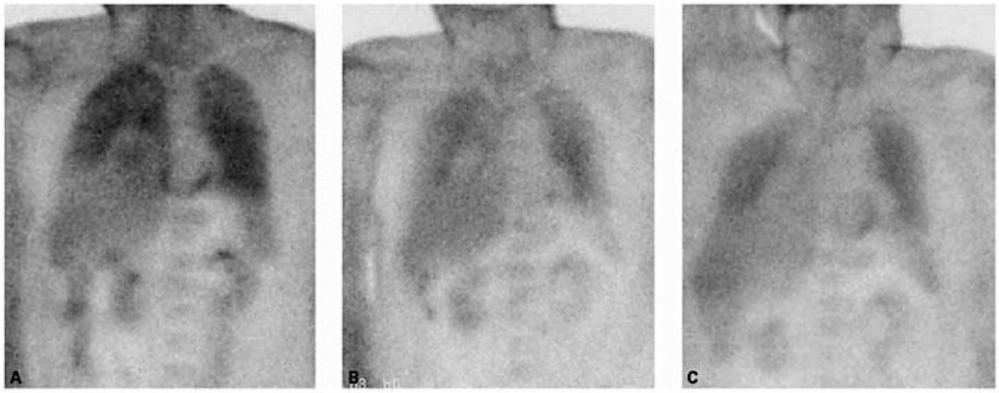

Figure 4. A. Baseline FDG-PET scan obtained on a 56 year old patient with lung infection. There is apparently increased uptake of FDG in the lung compared to the liver; **B.** Repeat FDG-PET scan after 3 months of treatment with high-dose antibiotics. Lung uptake has decreased in intensity and is very similar to the uptake by the liver; **C.** FDG-PET obtained 3 months after reducing antibiotics with an associated increase in dyspnea. Lung uptake has increased compared to the last study, Images reproduced with permission from [43], Copyright 2006, Karger Publishers.

3.1 Bacterial Pneumonia

Bacterial pneumonia is a type of pneumonia caused by bacterial infection. Gram positive bacteria including Streptococcus pneumoniae and Staphylococcus aureus are the most common bacterial cause of pneumonia in all age groups except newborn infants [37-39]. Several groups have reported to use FDG-PET/CT to evaluate distant metastatic infection and peripheral embolism in adult patients with infective bacterial pneumonia [40-42]. PET/CT [43] was also used in the case as the way of monitoring response to treatments (see Figure 4). This application is based on the ability of this technique to quantify the rate of FDG uptake. FDG-PET/CT therefore appears to be an effective tool to diagnose infection, monitor disease course and response to treatment in pneumonia. However, the overlap between FDG uptake of

ISSN 2291-6458 (Print), ISSN 2291-6466 (Online)
Year 2013 | Volume 1 | Issue 2 | Page 85-104

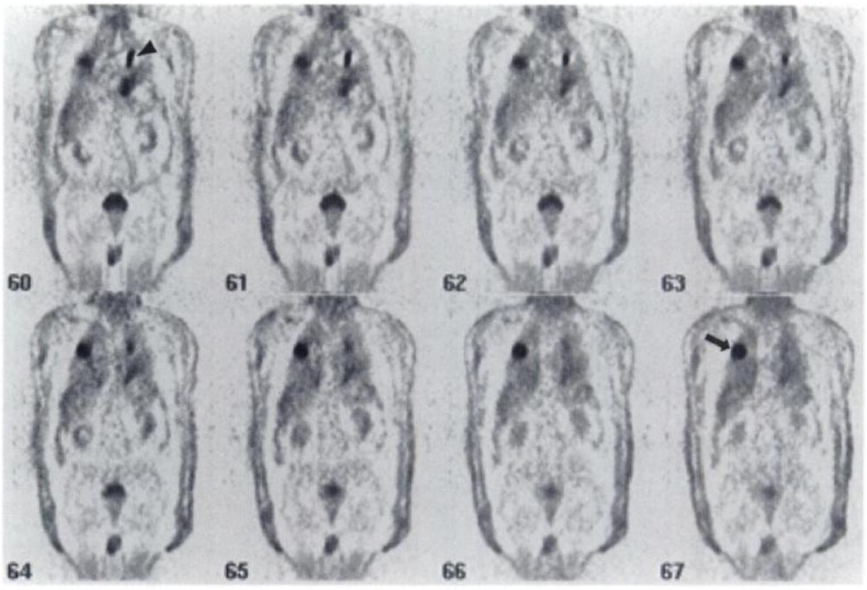

Figure 5. Eight sequential coronal whole-body FDG-PET images Show a large area of increased uptake in the right posterior upper lung (arrow). There is also an area of increased FDG uptake compatible with the patient's known malignancy in the left anterior upper lung (arrowhead). SUVs of lesions were 4.9 and 5.4, respectively, Images reproduced with permission from [46], Copyright 1998, SNMMI.

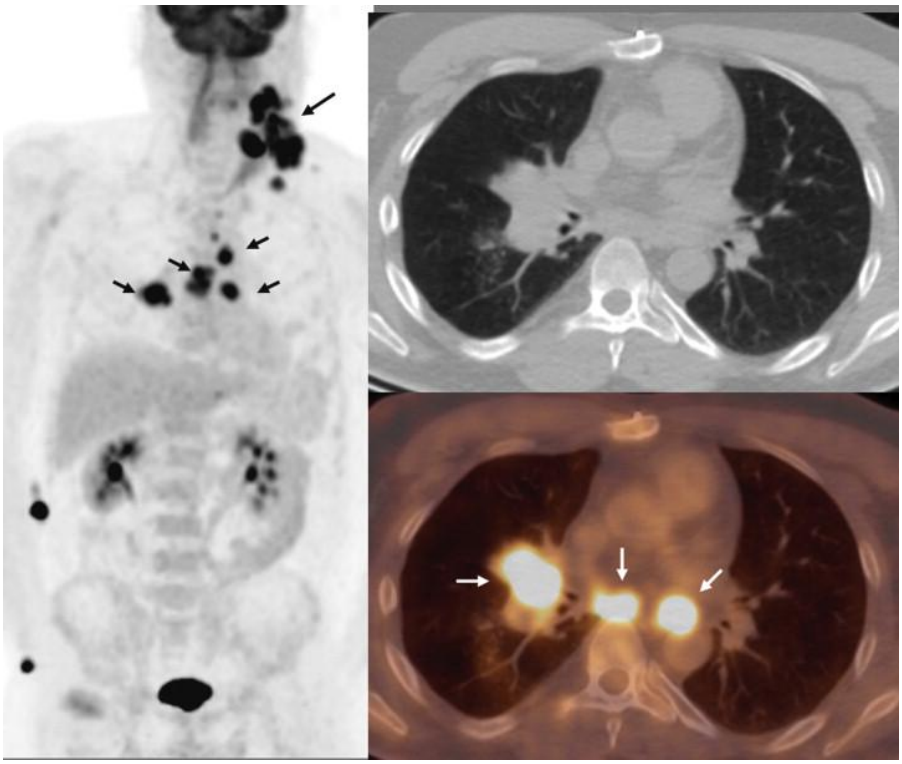

Figure 6. FDG-PET/CT in a 54-year-old man with a suspicion of tuberculosis. The lymphatic pattern was observed with a right hilum FDG uptake associated with enlarged and FDG avid asymmetric mediastino hilar and left cervical lymph nodes. *Mycobacterium tuberculosis* was diagnosed on cervical lymph node biopsy cultures, Images reproduced with permission from [47], Copyright 2012, Elsevier.

ISSN 2291-6458 (Print), ISSN 2291-6466 (Online)
Year 2013 | Volume 1 | Issue 2 | Page 85-104

malignant lesions and severe infectious pneumonia may limit the use of FDG-PET as a diagnostic tool in evaluation of infectious processes [44,45]. For example, FDG-PET scans show that both bacterial pneumonia with markedly elevated FDG uptake in a patient with concomitant squamous cell carcinoma in the contralateral lung. The FDG standardized uptake values (SUVs) were similar [46] for both lesions (4.9 and 5.4) (Figure 5). This case demonstrates that an inflammatory etiology for false-positive FDG-PET imaging in the evaluation of pulmonary abnormalities is necessary.

3.2 Tuberculosis (TB)

Tuberculosis is one of the most deadly diseases that cause more than a million people dead each year and infects half of the world population. Owing to its airborne transmission, early diagnosis is critical for the prevention of TB and can dramatically reduce the TB associated mortality and mobility [48-50]. FDG-PET/CT has been reported in detection of unsuspected infection foci and characterizing the structural lesions. FDG-PET/CT [47] showed that there was intense multifocal uptake in mediastinal, supraclavicular, and para-aortic areas that was confirmed radiologically to represent widespread lymphadenopathy (Figure 6). Pathologic examination of a mediastinal lymph node showed active tuberculosis. In addition, there was abnormal F-18 FDG lung uptake that revealed the presence of tuberculosis on bronchial lavage [51]. Furthermore, F18-FDG-PET/CT is also useful to know the extent of the disease [47]. These findings illustrate the potential application of FDG-PET/CT in mapping active tuberculous lesions which can be used for baseline study. However, FDG-PET does not behave in any characteristic manner in these conditions with the tuberculous lesion showing variable FDG uptake according to the grade of inflammatory activity [47]. Therefore, biopsy and histopathological examination may still be essential in many other cases for final diagnosis. In addition, whether FDG-PET is applicable in follow up of patients with known tuberculosis for response to treatment evaluation [52] remains to be studied (Figure 7).

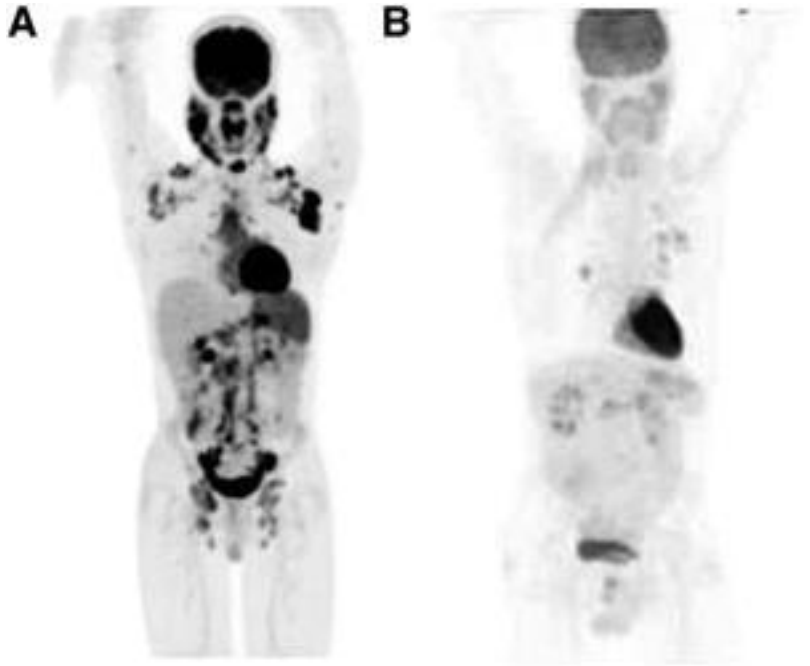

Figure 7. The use of FDG-PET scans can help to diagnose tuberculosis (A) and determine earlier that the treatment for tuberculosis is working (B), Images reproduced with permission from [52], Copyright 1998, SNMMI.

ISSN 2291-6458 (Print), ISSN 2291-6466 (Online)
Year 2013 | Volume 1 | Issue 2 | Page 85-104

3.3 Osteomyelitis

Osteomyelitis (OM) is infection and inflammation of the bone or bone marrow and usually is cause by either pyogenic bacteria or mycobacteria. Although some radionuclide imaging technologies have been used to diagnose osteomyelitis, such as three-phase bone scintigraphy, dual radiotracer studies combined sequential bone-gallium and leukocyte–bone marrow imaging and labeled leukocyte imaging, all of them have limited impact on clinical diagnosis due to difficult performing, high cost, inconvenience and unavailability [53]. FDG-PET/CT exhibits its strong competition in the diagnosis of osteomyelitis because FDG uptake by normal cortical bone is quite low, and bone marrow uptake is variable and can be slightly to moderately more intense than that of bone. Several studies [54-56] have shown that FDG is effective in diagnosing osteomyelitis (Figure 8). It is highly sensitive for detection of chronic osteomyelitis, even in patients treated with antibiotics before they undergo FDG-PET imaging [54-56]. FDG-PET was also advantageous to diagnose osteomyelitis in special situations like trauma, surgery and after other interventions where is difficult for existing radiological or nuclear medicine techniques to accurately diagnose chronic osteomyelitis. However, increased osseous FDG accumulation [53,57] has been observed in inflammatory arthritis, in acute fractures, and in normally healing bone after surgery (Figure 9). These observations are not surprising: The healing process is associated with many of the same cellular components that are present in inflammation. Thus extensive investigations focusing on specific indications are needed to accurately define the role of FDG-PET in the evaluation of Osteomyelitis.

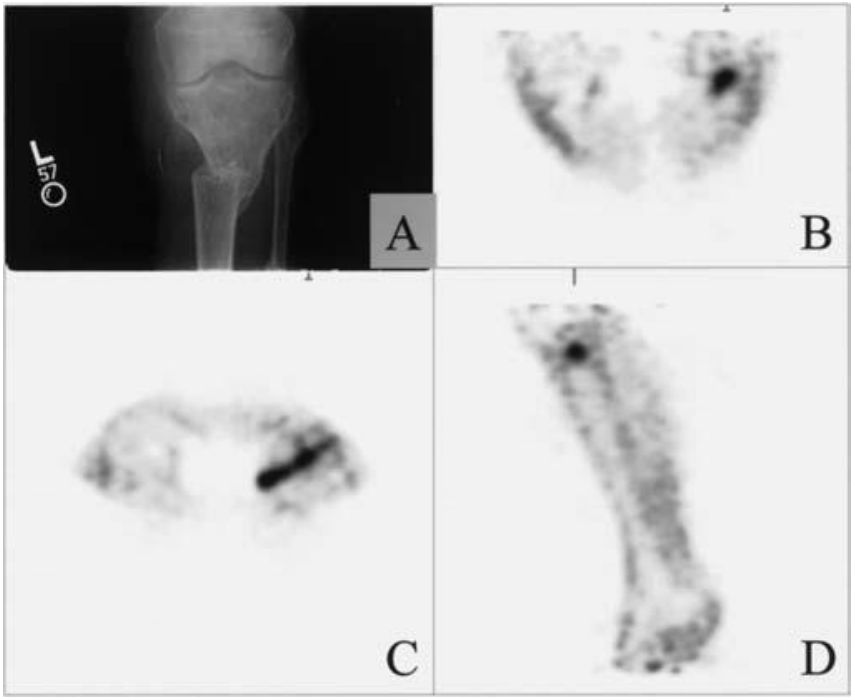

Figure 8. Images of a 54-year-old female with a history of left tibia fracture (A plain radiograph) due to motor vehicle accident 18 months prior to FDG-PET study. FDG-PET images (B coronal image, C transaxial image, D sagittal image) revealed a tract of significantly increased FDG accumulation. A portion of the abnormal activity was inside the cavity of the left proximal tibia. Bone biopsy demonstrated that the patient had chronic osteomyelitis, Images repproduced from [56], Copyright 2003, Springer.

ISSN 2291-6458 (Print), ISSN 2291-6466 (Online)
Year 2013 | Volume 1 | Issue 2 | Page 85-104

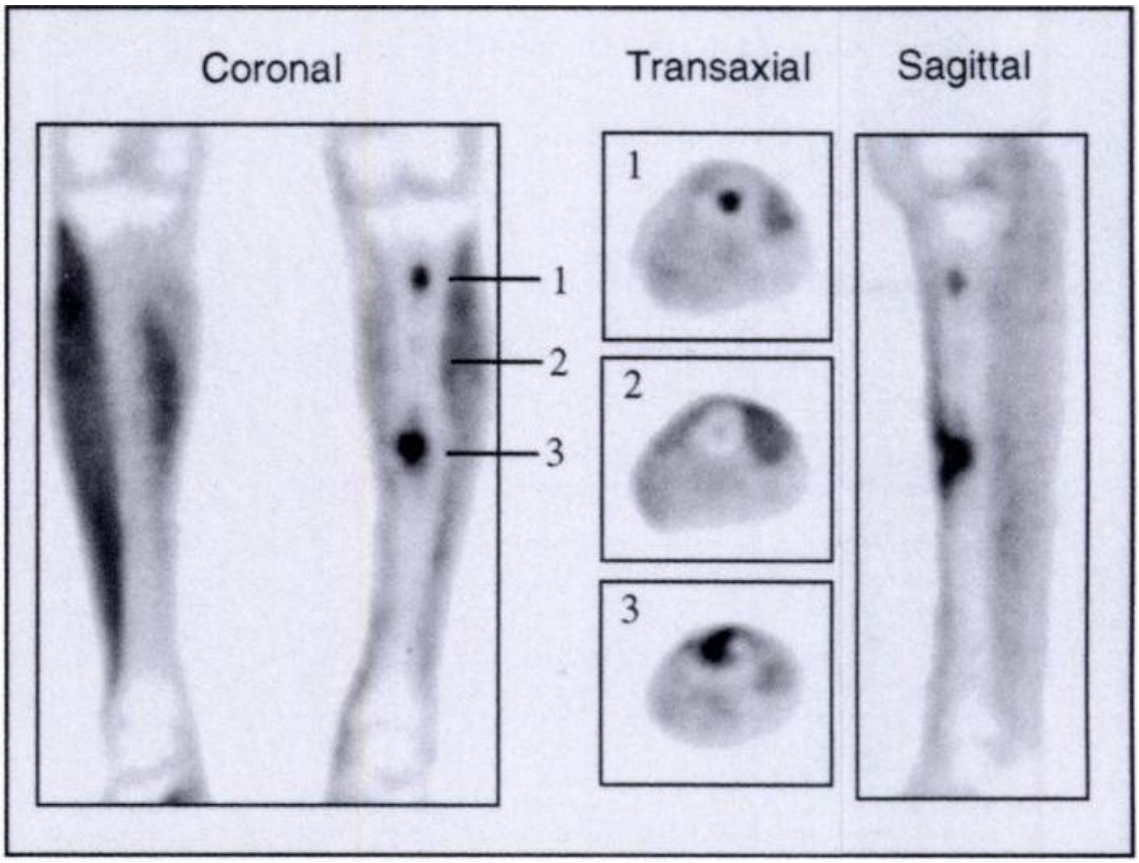

Figure 9. Chronic osteomyelitis of the proximal left tibia after trauma in a 36-year-old man. FDG-PET images show FDG uptake has been observed in both osteomyelitis and inflammatory arthritis, Images reproduced with permission from [57], Copyright 1998, RSNA.

3.4 Infected Prosthesis

About half a million of Americans are received hip and knee arthroplasties every year. Bacterial infection is the most common cause of joint arthroplasty failure [58]. The diagnosis of infection has significant implications, both clinically and economically, in terms of prolonged antibiotic treatment, a longer hospital stay, and a second operation. The failure to diagnose infection will lead to failure of a revision arthroplasty, continuing periprosthetic osteolysis, and the need for a second surgical procedure, which may be more difficult and extensive than the first. In most patients, multiple tests are required to establish the diagnosis before revision surgery, and all of them have limited sensitivity and specificity [58]. The role of FDG-PET in the evaluation of painful lower extremity joint prostheses has been extensively investigated [59,60]. Initial reports [61] suggested that FDG-PET has excellent sensitivity but low specificity for imaging periprosthetic infection (Figure 10). Recent studies show that FDG-PET can prove prosthetic infection in hip implants with more than 90% accuracy [60]. However, non-specific increased FDG uptake was also observed in the prosthesis without any complications and sterile inflammation induced by surgery. In addition, FDG-PET [61]does not appear to be capable of helping to distinguish an infected joint prosthesis from an aseptically loosened prosthesis (Figure 11). Therefore, more studies are needed to confirm the role of FDG-PET in the evaluation of periprosthetic infection or inflammation [59,60].

ISSN 2291-6458 (Print), ISSN 2291-6466 (Online)
Year 2013 | Volume 1 | Issue 2 | Page 85-104

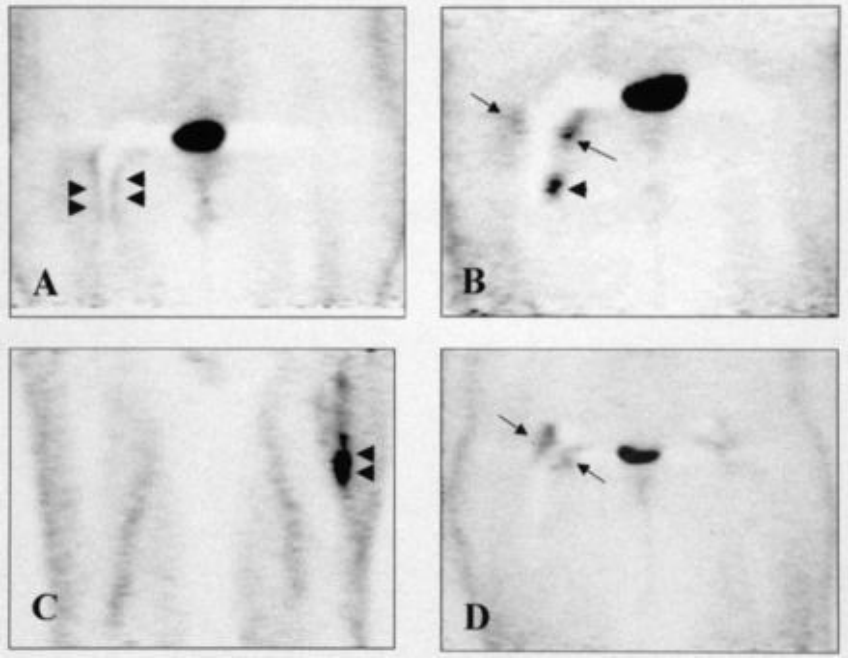

Figure 10. (A) Coronal image of 72-y-old woman with hip prosthesis. Periprosthetic infection on right side was identified (arrowheads). (B) Coronal image of 76-y-old woman with bilateral hip prostheses. Both infection (arrowhead) and loosening (arrows) were shown. (C) Coronal image of 78-y-old man with painful left hip prosthesis. Arrowheads indicate periprosthetic infection and osteomyelitis. (D) Coronal image of 76-y-old woman with bilateral hip prostheses. FDG uptake is noted only around neck of prosthesis (arrows). FDG PET diagnosis of loosening was confirmed after revision arthroplasty, Images reproduced with permission from [59], Copyright 2001, SNMMI.

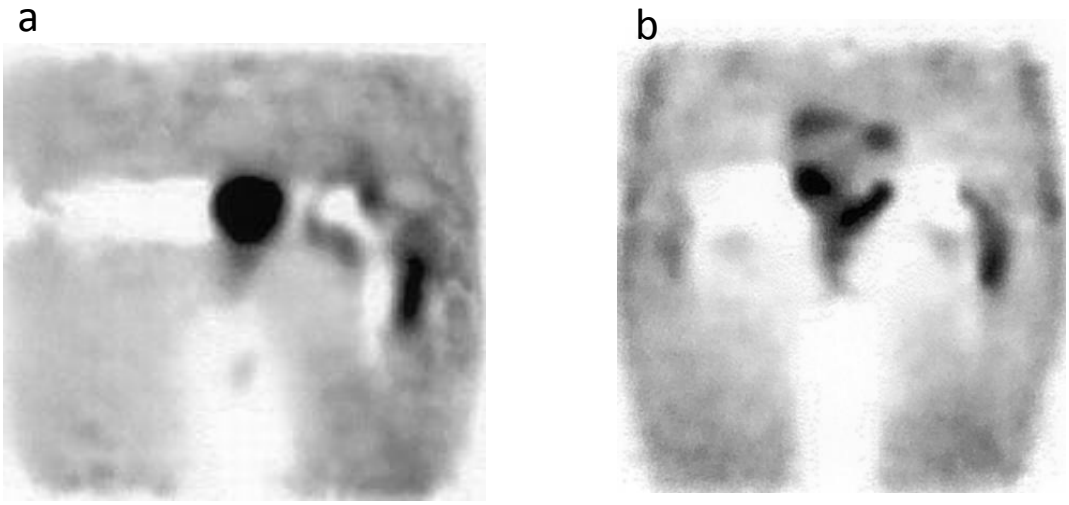

Figure 11. (a) Infected left hip prosthesis. FDG-PET scan shows increased periprosthetic radiotracer activity at the bone-prosthesis interface along the lateral aspect of the femoral component of the prosthesis. **(b)** Aseptically loosened left hip prosthesis. FDG-PET scan demonstrates uptake similar to that seen in (**a**) along the lateral margin of the prosthesis. Bone-prosthesis interface activity at FDG-PET, once thought to be specific for infection, is probably related to osteolysis, which is present in both infection and loosening, Images reproduced with permission from [61], Copyright 2004, SNMMI.

ISSN 2291-6458 (Print), ISSN 2291-6466 (Online)
Year 2013 | Volume 1 | Issue 2 | Page 85-104

3.5 Diabetic Foot Infection

Diabetes mellitus occurs throughout the world, and more than 200 million people have diabetes in the world [55]. Foot infection frequently coexist in diabetic patients, and cause serious mal perforans ulcer, which accounts for more than 90% of all cases of diabetic pedal osteomyelitis. Diagnosis of osteomyelitis via radiography, CT or MRI is limited because of lack of specificity and incapability of distinguishing between infection and neuropathic osteoarthropathy of the foot, which normally coexist in diabetic patients [53]. ^{111}In-oxine labeled white blood cell (WBC) imaging is most popular diagnostic method for diabetic pedal osteomyelitis, and has sensitivities ranging from 72% to 100% and specificities ranging from 67% to 100% [53,62]. However, WBC imaging is difficult to differentiate soft tissue from bone infection because poor spatial resolution and lack of bony landmarks [53,62]. FDG-PET/CT shows high sensitivity to excluding osteomyelitis in the diabetic foot because the precise anatomic localization of increased FDG uptake provided by PET/CT enables accurate differentiation between osteomyelitis and soft-tissue infection [55]. The reported studies [63] displays that FDG-PET/CT could play a role in assessing complicated and uncomplicated diabetic osteoarthropathy, being able to provide accurate assessment of patients with metal implants who may not be suitable candidates for MRI, and to correctly distinguish osteomyelitis from neuroarthropathy (Figure 12). However, in a recent prospective study conducted in 110 patients with complicated diabetic foot, FDG-PET/CT was found to be a low specific imaging modality for the diagnosis of osteomyelitis [64]. These findings suggest that FDG-PET/CT cannot yet replace WBC imaging.

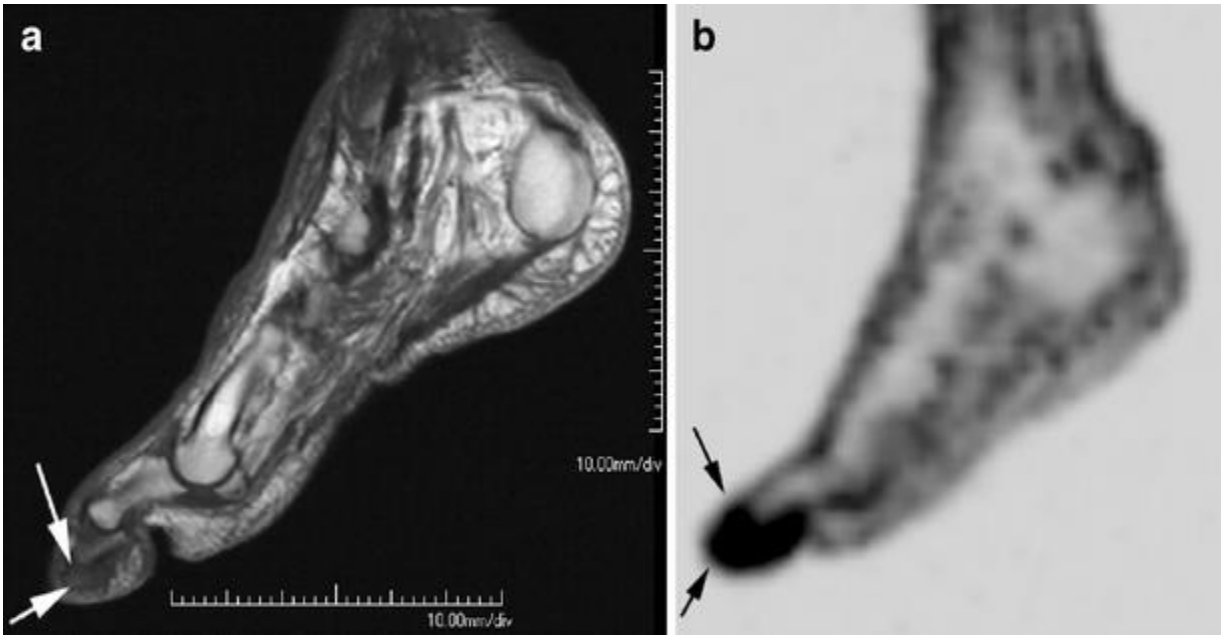

Figure 12. Fifty-year-old diabetic male presented with an ulcer of the right great toe. **a** T1-weighted sagittal magnetic resonance image of the right foot demonstrates loss of signal intensity in the great toe region suggestive of osteomyelitis. **b** PET also demonstrates enhanced uptake of FDG at the corresponding site of abnormality as noted on magnetic resonance imaging. This further confirms the diagnosis of osteomyelitis in the great toe, Images reproduced from [63], Copyright 2009, Springer.

3.6 Vertebral Osteomyelitis

Vertebral osteomyelitis is a rare bone infection concentrated in the spinal region and has a predilection for young children and older adults. Vertebral osteomyelitis often attacks two vertebrae and the corresponding intervertebral disk, causing narrowing of the disc space between the vertebrae [65].

ISSN 2291-6458 (Print), ISSN 2291-6466 (Online)
Year 2013 | Volume 1 | Issue 2 | Page 85-104

The prognosis for the disease is dependent on where the infection is concentrated in the spine, the time between initial onset and treatment, and what approach is used to treat the disease. MRI is the major diagnostic method for spinal osteomyelitis, and has an accuracy of more than 90% [66]. MR imaging permits early diagnosis of infection and provides direct visualization of the spinal cord, subarachnoid space and extradural soft tissues. However, MRI is not suitable for the patients with metallic implants and cannot distinguish osteomyelitis from severe degenerative arthritis. The current radionuclide imaging method for diagnosing spinal osteomyelitis, such as gallium single photon emission CT (SPECT), is time consuming and requires multiple scans [67]. Recently, FDG-PET/CT [68,69] has been used to diagnose vertebral osteomyelitis and appears high sensitivities and specificities (Figure 13 and Figure 14). Although only few studies have been reported, FDG-PET/CT shows accuracy comparable to that of gallium imaging, indicating that it could be applicable in diagnosing spinal osteomyelitis.

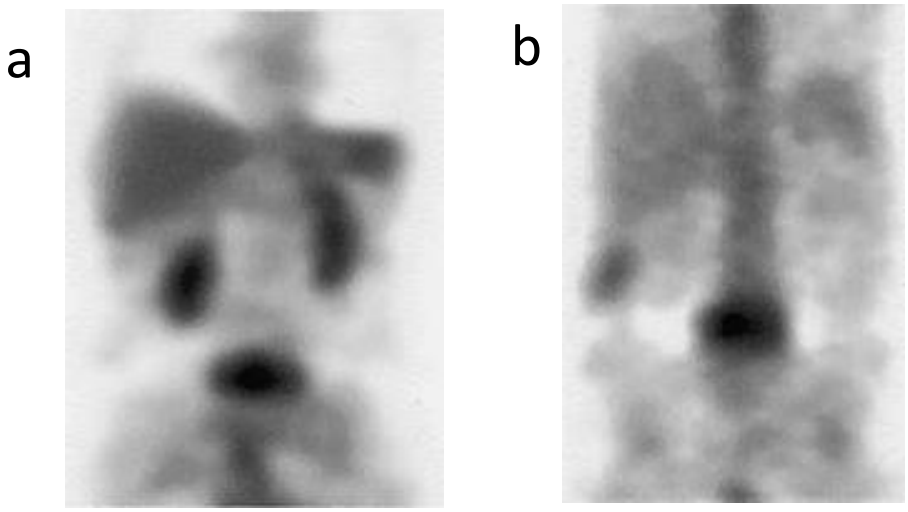

Figure 13. Spinal osteomyelitis. **(a)** FDG-PET scan shows intense radiotracer accumulation in the lower lumbar spine. **(b)** Coronal image from a gallium SPECT study shows a similar abnormality, Images reproduced with permission from [68], Copyright 2006, Elsevier.

3.7 Bacterial Endocarditis

Bacterial endocarditis is an infection or inflammation of the inner layer of the heart, the endocardium, and is a common cause of morbidity and mortality in the United States. Normally, Echocardiography (EC) plays a major role in diagnosing and monitoring the therapeutic response in infective endocarditis (IE) in routine practice [70]. However in the setting of prosthetic valves or indwelling pacemakers, the EC findings are equivocal necessitating search for other diagnostic modalities. Although the diagnosis of infective endocarditis with a variety of radionuclide imaging techniques has been reported, the clinical value of these techniques has never been established [71]. A recent study [72] shows that FDG-PET imaging can truthfully help identify sites of infective endocarditis in an 82 years old male with a mechanical aortic valve prosthesis who presented with a 10 days history of fever and malaise (Figure 15). Optimal interpretation of the EC results was difficult due to the presence of the prosthetic valve. However, FDG-PET imaging findings were quite distinctive and revealed abnormally increased metabolic activity represented by two foci corresponded to areas of bacterial endocarditis. These studies [73] indicate that FDG-PET is a promising supplement to conventional echocardiography (Figure 16).

ISSN 2291-6458 (Print), ISSN 2291-6466 (Online)
Year 2013 | Volume 1 | Issue 2 | Page 85-104

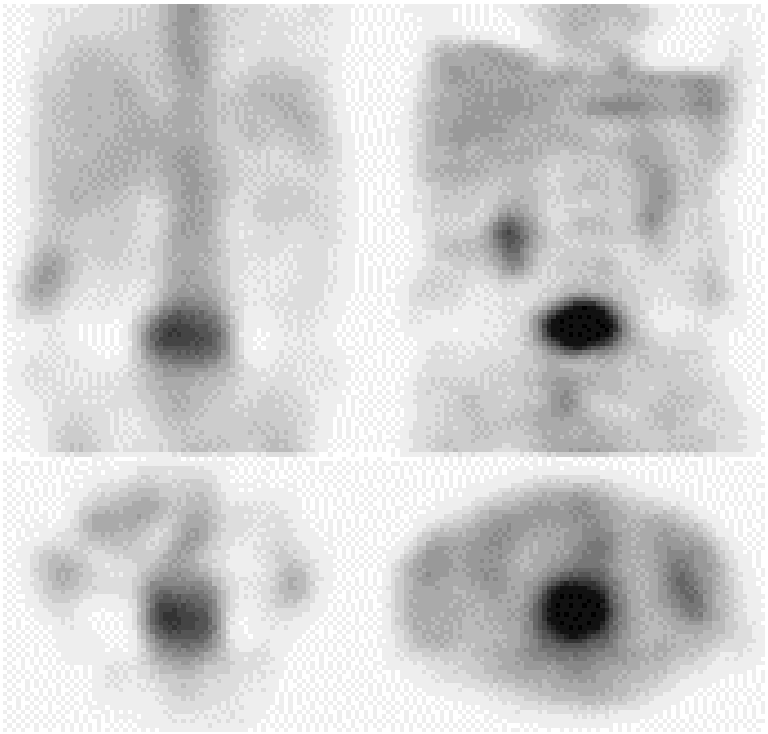

Figure 14. Spinal osteomyelitis. Both the gallium (*left*) and FDG-PET (*right*) images demonstrate intensely increased activity in a focus of osteomyelitis of the lumbar spine. Gallium study was performed about 48 hours after tracer injection; FDG-PET about one hour after injection, Images reproduced from [69], Copyright 2002, Springer.

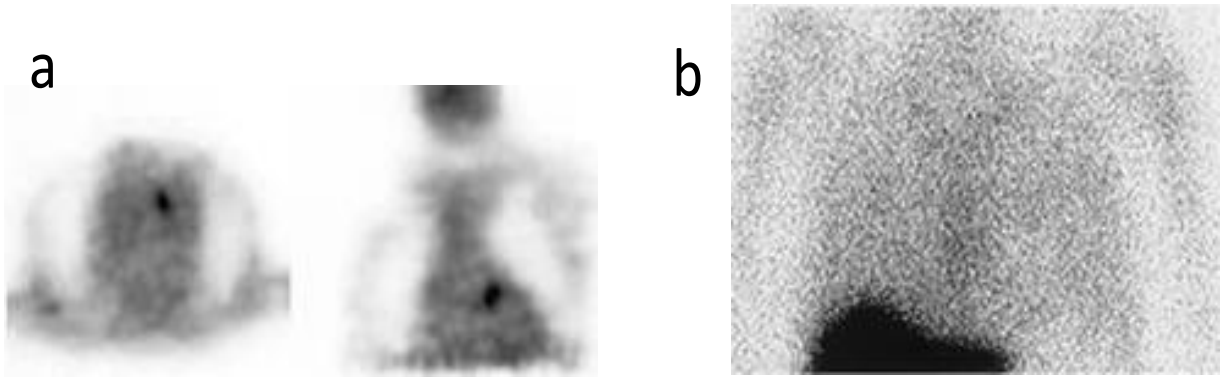

Figure 15. Infective endocarditis in a patient who had undergone mitral valve replacement. FDG-PET was performed because of persistent bacteremia. **(a)** Axial (left) and coronal (right) FDG-PET scans show a focus of increased intracardiac activity. Results of echocardiography confirmed the presence of valvular vegetations and a mitral annular abscess. **(b)** ^{111}In-labeled leukocyte image is unremarkable, Images reproduced with permission from [72], Copyright 2002, Elsevier.

3.8 Fever of Undetermined Origin (FUO)

FUO refers to a condition in which the patient has an elevated temperature but no diagnosis has been concluded after investigations by a physician. There are several causes of FUO, and infection are one of the most frequent origins followed by neoplasm, and other sterile inflammatory diseases [74]. The

ISSN 2291-6458 (Print), ISSN 2291-6466 (Online)
Year 2013 | Volume 1 | Issue 2 | Page 85-104

accurate diagnosis of the cause of FUO will undoubtedly improve the treatment of these patients. However, identification of the source of an FUO is often challenged, and radio imaging is an important part of the diagnostic method [75]. FDG- PET has the potential to take a part in the diagnostic protocol and management of patients with FUO because of high sensitivity of FDG-PET in detecting malignant lesions, infection, and various inflammatory processes. Furthermore, the short half-life of ^{18}F does not delay the performance of any additional radionuclide studies that might be anticipated. Indeed, there are several studies that support the use of FDG-PET in patients with FUO [76-79]. For example, a recent study [80] analyzed the value of FDG-PET/CT in patients with FUO or unexplained signs of inflammation without fever and found the technique to be a valuable diagnostic tool in these subjects in whom a non-traumatic method of depicting inflammation in the whole body is obviously particularly useful (Figure 17). The data show that FDG-PET is helpful in most cases, and has the sensitivity ranging from 77% to 92% and specificities ranging from 89% to 100%. FDG-PET/CT has proven applicable in the initial diagnosis of patients suspected of having UFO, particularly those who present with non-specific symptoms, in the identification of areas of increased FDG uptake requiring biopsy, and in the evaluation

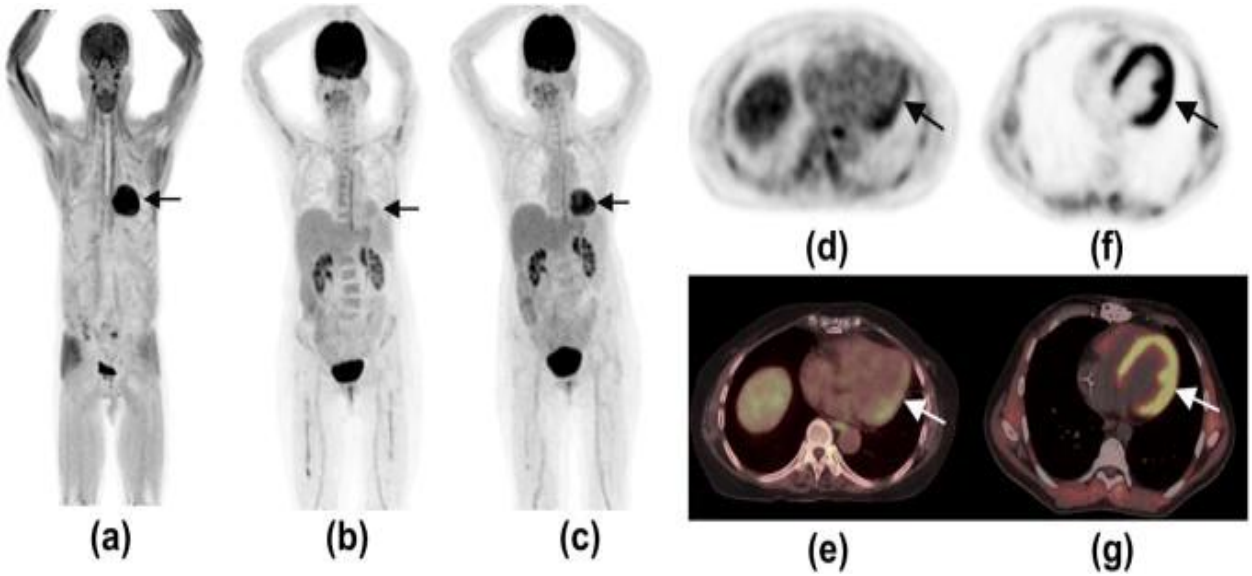

Figure 16. (a) Anterior FDG-PET maximum intensity projection (MIP) image in a 33-year-old female patient with lymphoma shows FDG bio-distribution that indicates a non-fasting state. The patient did not adhere to the fasting preparation and consequently has peripheral muscle FDG distribution, low cerebral FDG uptake, and intense cardiac FDG uptake (arrow) reflecting elevated plasma glucose and insulin levels. (b, c) Anterior FDG-PET MIP images in a 74-year-old female performed 2 months apart demonstrate temporally and spatially variable cardiac FDG uptake in the same patient (arrows). (d, e) Axial PET and fusion PET images show regional lateral LV myocardial uptake (arrows), a well-described physiological variant that occurs despite adequate fasting. (f, g) Axial PET and fusion PET images show diffuse LV myocardial uptake (arrows), a physiological variant that is encountered in fasted patients, Images reproduced with permission from [73], Copyright 2010, Elsevier.

of the extent of disease [81]. All these studies stress the advantages of FDG-PET/CT for evaluating patients with FUO. However, calculation of the sensitivity and specificity of FDG-PET in patients with FUO [82] is difficult due to the lack of a gold standard because a final diagnosis is not established in all patients (Figure 18). Moreover, FDG is a radiopharmaceutical that accumulates in infection, malignancies and inflammatory diseases. This non-specificity makesit impossible to discriminate between infection and neoplastic disease [76]. Therefore, there is a need of developing a structured

ISSN 2291-6458 (Print), ISSN 2291-6466 (Online)
Year 2013 | Volume 1 | Issue 2 | Page 85-104

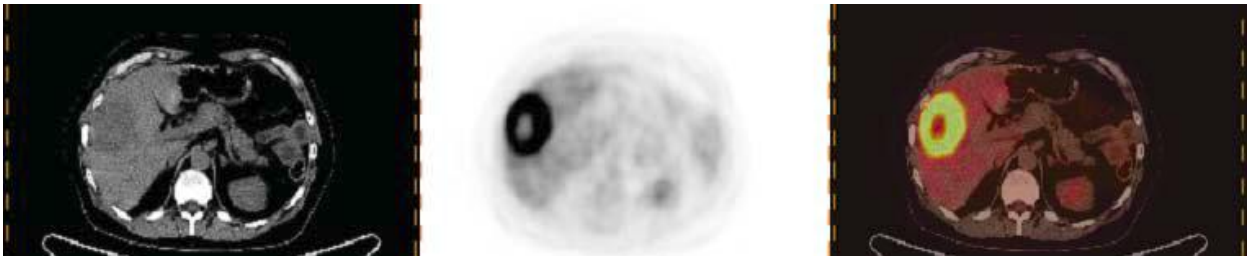

Figure 17. Patient of liver abscess underwent PET-CT scan. PET-CT shows intense FDG uptake in the periphery of lesion with no uptake in center of the right lobe liver lesion (doughnut appearance) suggestive of central necrosis, Images reproduced with permission from [80], Copyright 2011, RSNA.

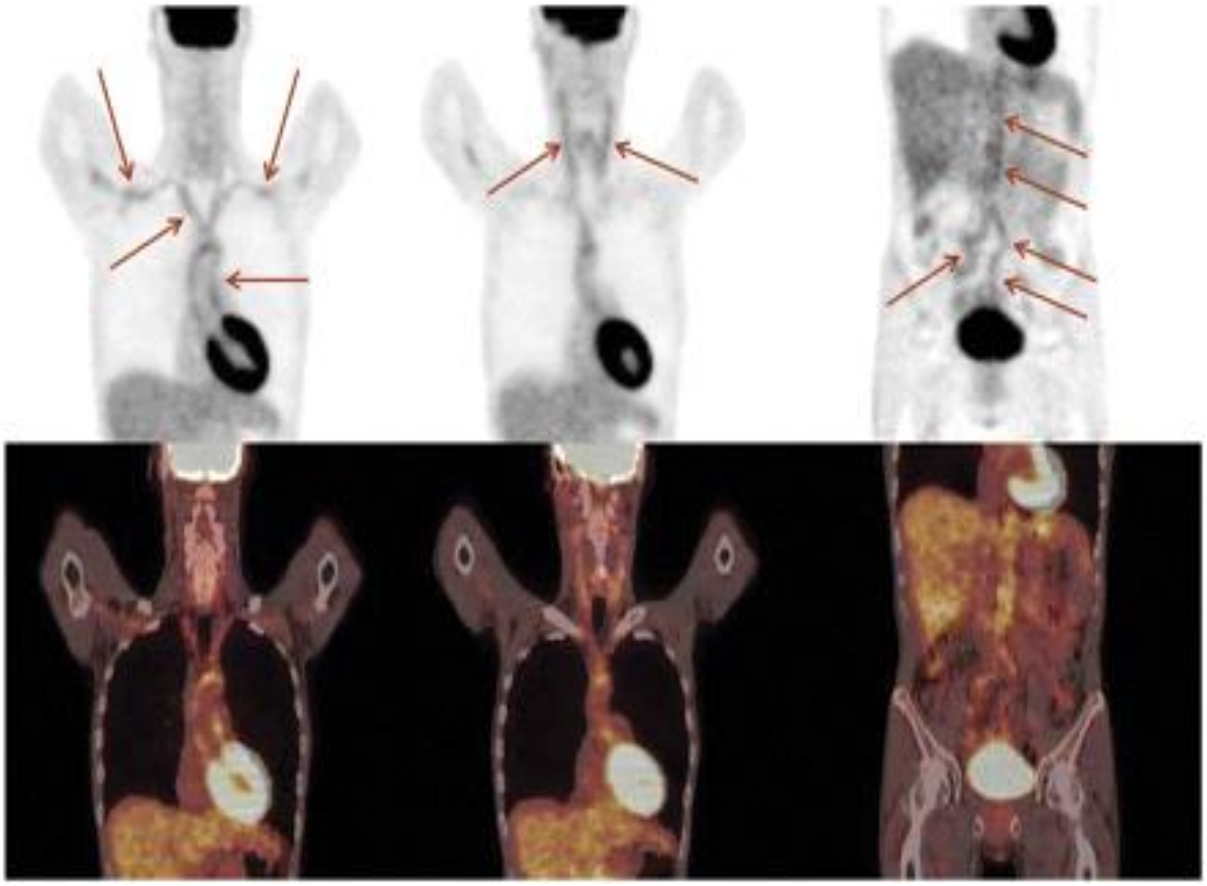

Figure 18. Patient with a history of FUO. Physical examination and ultrasonography of temporal artery were negative. Erythrocyte sedimentation and C-reactive protein were elevated; otherwise, laboratory parameters did not indicate vasculitis. FDG PET scan shows increased uptake in thoracic aorta and subclavian arteries (left), carotid arteries (middle), and abdominal aorta together with iliac arteries (right) (arrows). Vasculitis was diagnosed. This example demonstrates that PET has the potential for detection of vasculitis as underlying cause of FUO, Images reproduced with permission from [82], Copyright 2010, SNMMI.

ISSN 2291-6458 (Print), ISSN 2291-6466 (Online)
Year 2013 | Volume 1 | Issue 2 | Page 85-104

diagnostic protocol for FDG-PET/CT imaging, which will help to identify the source organ or tissue of the fever, thereby guiding additional, appropriate testing. The application of FDG-PET/CT in diagnosis of patients with FUO is growing and this technique is probably destined to become the preferred diagnostic procedure in the future, especially when a definite diagnosis cannot easily be achieved.

4. CONCLUSIONS

There is a great need of developing an ideal diagnostic method for bacterial infection in the clinic. FDG-PET fulfills the most criteria established for molecular imaging, and appears to be a potential powerful tool in the diagnosis of infection. Although the use of FDG-PET may be limited because of the lack of specificity and its incapability of discriminating bacterial infection from other inflammatory disorders, it has already had a highly impact on diagnosis, staging of bacterial infection and evaluation of therapy and will definitely take a part in the diagnosis and management of inflammatory or infectious diseases.

REFERENCES AND NOTES

[1] Handrick, W.; Spencker, F. B.; Braun, W.; Springer, W.; Boehm, G.; Scheerschmidt, G.; Mahnke, P. F.: [Bacterial infections developing outside of the clinic in the first month of life]. *Kinderarztl. Prax.* **1987**, *55*, 139-45.

[2] Cao, W. B.; Su, D.; Chen, Y. M.; Zheng, Y. Z.; Zhang, F. K.; Feng, S. Z.; Han, M. Z.: [Clinical features and antimicrobial resistance of Gram positive bacterial blood stream infection in patients with hematologic diseases]. *Zhonghua xue ye xue za zhi* **2012**, *33*, 566-9.

[3] Heineman, J.; Bubenik, S.; McClave, S.; Martindale, R.: Fighting fire with fire: is it time to use probiotics to manage pathogenic bacterial diseases? *Curr. gastroenterol. rep.* **2012**, *14*, 343-8.

[4] Kemp, M.; Dargis, R.; Andresen, K.; Christensen, J. J.: A program against bacterial bioterrorism: improved patient management and acquisition of new knowledge on infectious diseases. *Biosecur. Bioterror.* **2012**, *10*, 203-7.

[5] Konieczna, I.; Zarnowiec, P.; Kwinkowski, M.; Kolesinska, B.; Fraczyk, J.; Kaminski, Z.; Kaca, W.: Bacterial urease and its role in long-lasting human diseases. *Curr. Protein Pept. Sci.* **2012**, *13*, 789-806.

[6] Gratz, S.; Rennen, H. J.; Boerman, O. C.; Oyen, W. J.; Corstens, F. H.: Rapid imaging of experimental colitis with (99m)Tc-interleukin-8 in rabbits. *J. Nucl. Med.* **2001**, *42*, 917-23.

[7] Lupetti, A.; Welling, M. M.; Pauwels, E. K.; Nibbering, P. H.: Radiolabelled antimicrobial peptides for infection detection. *Lancet Infect. Dis.* **2003**, *3*, 223-9.

[8] Signore, A.; Annovazzi, A.; Corsetti, F.; Capriotti, G.; Chianelli, M.; De Winter, F.; Scopinaro, F.: Biological imaging for the diagnosis of inflammatory conditions. *BioDrugs* **2002**, *16*, 241-59.

[9] Kirchner, J.; Kickuth, R.; Stein, A.; Kirchner, E. M.: [Mesenteric ossification in CT indicates sclerosing peritonitis in chronic bacterial infection and pancreatitis]. *Rontgenpraxis* **2003**, *55*, 99-102.

[10] Winklhofer, S.; Kollias, S.: Incidental MRI finding of a pons tuberculoma in a patient with so-far-undiagnosed multisystemic tuberculosis infection. *Clin. Imag.* **2012**, *36*, 623-625.

[11] Palestro, C. J.; Love, C.; Tronco, G. G.; Tomas, M. B.: Role of radionuclide imaging in the diagnosis of postoperative infection. *Radiographics* **2000**, *20*, 1649-60; discussion 1660-3.

[12] Peters, A. M.: Nuclear medicine imaging in infection and inflammation. *J. R. Coll. Physicians Lond.* **1998**, *32*, 512-9.

[13] Haubner, R.: PET radiopharmaceuticals in radiation treatment planning - synthesis and biological characteristics. *Radiother. Oncol.* **2010**, *96*, 280-7.

[14] Fletcher, J. W.; Djulbegovic, B.; Soares, H. P.; Siegel, B. A.; Lowe, V. J.; Lyman, G. H.; Coleman, R. E.; Wahl, R.; Paschold, J. C.; Avril, N.; Einhorn, L. H.; Suh, W. W.; Samson, D.; Delbeke, D.; Gorman, M.;

ISSN 2291-6458 (Print), ISSN 2291-6466 (Online)
Year 2013 | Volume 1 | Issue 2 | Page 85-104

Shields, A. F.: Recommendations on the use of 18F-FDG PET in oncology. *J. Nucl. Med.* **2008**, *49*, 480-508.

[15] Chen, S. H.; Ho, K. C.; Hsieh, P. H.; Lee, M. S.; Yen, T. C.: Potential clinical role of 18F FDG-PET/CT in detecting hip prosthesis infection: a study in patients undergoing two-stage revision arthroplasty with an interim spacer. *Q. J. Nuc.l Med. Mol. Imaging* **2010**, *54*, 429-35.

[16] Dumarey, N.; Egrise, D.; Blocklet, D.; Stallenberg, B.; Remmelink, M.; del Marmol, V.; Van Simaeys, G.; Jacobs, F.; Goldman, S.: Imaging infection with 18F-FDG-labeled leukocyte PET/CT: initial experience in 21 patients. *J. Nucl. Med.* **2006**, *47*, 625-32.

[17] Sato, M.; Hiyama, T.; Kaito, K.; Hayashi, Y.; Okumura, T.: Usefulness of F-18 FDG PET/CT in the assessment of disseminated Mycobacterium avium complex infection. *Ann. Nucl. Med.* **2009**, *23*, 757-62.

[18] Vos, F. J.; Bleeker-Rovers, C. P.; Sturm, P. D.; Krabbe, P. F.; van Dijk, A. P.; Cuijpers, M. L.; Adang, E. M.; Wanten, G. J.; Kullberg, B. J.; Oyen, W. J.: 18F-FDG PET/CT for detection of metastatic infection in gram-positive bacteremia. *J. Nucl. Med.* **2010**, *51*, 1234-40.

[19] Bida, G. T.; Satyamurthy, N.; Barrio, J. R.: The Synthesis of 2-[F-18]Fluoro-2-Deoxy-D-Glucose Using Glycals - a Reexamination. *J. Nucl. Med.* **1984**, *25*, 1327-1334.

[20] Fowler, J. S.; Ido, T.: Initial and subsequent approach for the synthesis of 18FDG. *Semin. Nucl. Med.* **2002**, *32*, 6-12.

[21] Ehrenkaufer, R. E.; Potocki, J. F.; Jewett, D. M.: Simple Synthesis of F-18-Labeled 2-Fluoro-2-Deoxy-D-Glucose - Concise Communication. *J. Nucl. Med.* **1984**, *25*, 333-337.

[22] Szarek, W. A.; Hay, G. W.; Perlmutter, M. M.: A Rapid, Stereospecific Synthesis of 2-Deoxy-2-Fluoro-D-Glucose Using the Fluoride-Ion. *J. Chem. Soc. Chem. Comm.* **1982**, 1253-1254.

[23] Hamacher, K.; Coenen, H. H.; Stocklin, G.: Efficient stereospecific synthesis of no-carrier-added 2-[18F]-fluoro-2-deoxy-D-glucose using aminopolyether supported nucleophilic substitution. *J. Nucl. Med.* **1986**, *27*, 235-8.

[24] Beeley, P. A.; Szarek, W. A.; Hay, G. W.; Perlmutter, M. M.: A Synthesis of 2-Deoxy-2-(F-18)Fluoro-D-Glucose Using Accelerator-Produced F-18 Fluoride Ion Generated in a Water Target. *Can. J. Chem.* **1984**, *62*, 2709-2711.

[25] Yu, S.: Review of F-FDG Synthesis and Quality Control. *Biomed. Imaging Interv. J.* **2006**, *2*, e57.

[26] Kubota, R.; Yamada, S.; Kubota, K.; Ishiwata, K.; Tamahashi, N.; Ido, T.: Intratumoral distribution of fluorine-18-fluorodeoxyglucose in vivo: high accumulation in macrophages and granulation tissues studied by microautoradiography. *J. Nucl. Med.* **1992**, *33*, 1972-80.

[27] Mochizuki, T.; Tsukamoto, E.; Kuge, Y.; Kanegae, K.; Zhao, S.; Hikosaka, K.; Hosokawa, M.; Kohanawa, M.; Tamaki, N.: FDG uptake and glucose transporter subtype expressions in experimental tumor and inflammation models. *J. Nucl. Med.* **2001**, *42*, 1551-5.

[28] Pauwels, E. K.; Ribeiro, M. J.; Stoot, J. H.; McCready, V. R.; Bourguignon, M.; Maziere, B.: FDG accumulation and tumor biology. *Nucl. Med. Bio.* **1998**, *25*, 317-22.

[29] Olson, A. L.; Pessin, J. E.: Structure, function, and regulation of the mammalian facilitative glucose transporter gene family. *Annu. Rev. Nutr.* **1996**, *16*, 235-56.

[30] Paik, J. Y.; Lee, K. H.; Choe, Y. S.; Choi, Y.; Kim, B. T.: Augmented 18F-FDG uptake in activated monocytes occurs during the priming process and involves tyrosine kinases and protein kinase C. *J. Nucl. Med.* **2004**, *45*, 124-8.

[31] Skillen, A.; Currie, G. M.; Wheat, J. M.: Thermal Control of Brown Adipose Tissue in 18F-FDG PET. *J. Nucl. Med. Technol.* **2012**, *40*, 99-103.

[32] Nakahara, T.; Fujii, H.; Ide, M.; Nishiumi, N.; Takahashi, W.; Yasuda, S.; Shohtsu, A.; Kubo, A.: FDG uptake in the morphologically normal thymus: comparison of FDG positron emission tomography and CT. *Br. J. Radiol.* **2001**, *74*, 821-4.

[33] Shreve, P. D.; Anzai, Y.; Wahl, R. L.: Pitfalls in oncologic diagnosis with FDG PET imaging: physiologic and benign variants. *Radiographics* **1999**, *19*, 61-77; quiz 150-1.

ISSN 2291-6458 (Print), ISSN 2291-6466 (Online)
Year 2013 | Volume 1 | Issue 2 | Page 85-104

[34] Cook, G. J.; Fogelman, I.; Maisey, M. N.: Normal physiological and benign pathological variants of 18-fluoro-2-deoxyglucose positron-emission tomography scanning: potential for error in interpretation. *Semin. Nucl. Med.* **1996**, *26*, 308-14.
[35] Yeung, H. W. D.; Grewal, R. K.; Gonen, M.; Schoder, H.; Larson, S. M.: Patterns of F-18-FDG uptake in adipose tissue and muscle: A potential source of false-positives for PET. *J. Nucl. Med.* **2003**, *44*, 1789-1796.
[36] Zhuang, H.; Alavi, A.: 18-fluorodeoxyglucose positron emission tomographic imaging in the detection and monitoring of infection and inflammation. *Semin. Nucl. Med.* **2002**, *32*, 47-59.
[37] Tan, K.; Lai, N. M.; Sharma, A.: Surfactant for bacterial pneumonia in late preterm and term infants. *Cochrane Database Syst. Rev.* **2012**, *2*, CD008155.
[38] Sachdev, A.; Chugh, K.; Raghunathan, V.; Gupta, D.; Wattal, C.; Menon, G. R.: Diagnosis of bacterial ventilator-associated pneumonia in children: reproducibility of blind bronchial sampling. *Pediatr. Crit. Care Med.* **2013**, *14*, e1-7.
[39] Chen, L. F.; Chang, C. Y.; Hsu, L. C.; Tsai, P. H.; Chang, S. J.; Chang, S. C.; Yuan, M. K.; Lai, Y. C.; Liu, Y. C.; Wang, W. S.: Bacterial pneumonia following acute ischemic stroke. *J. Chin. Med. Assoc.* **2013**, *76*, 78-82.
[40] Uruga, H.; Murase, R.; Kurosaki, A.; Ishihara, M.; Fujii, T.; Kishi, K.: [A case of caseous pneumonia demonstrating intense uptake on FDG-PET]. *Nihon Kokyuki Gakkai zasshi* **2010**, *48*, 247-52.
[41] Nakazato, T.; Mihara, A.; Sanada, Y.; Suzuki, K.; Aisa, Y.; Iwabuchi, M.; Kakimoto, T.: Pneumocystis jiroveci pneumonia detected by FDG-PET. *Ann. Hematol.* **2010**, *89*, 839-40.
[42] Bianco, A.; Mazzarella, G.; Rocco, D.; Gasperi, M.; Di Marco, R.; Brunese, L.: FDG/PET uptake in asymptomatic multilobar Chlamydia pneumoniae pneumonia. *Med. Sci. Monit.* **2010**, *16*, CS67-70.
[43] Meissner, H. H.; Soo Hoo, G. W.; Khonsary, S. A.; Mandelkern, M.; Brown, C. V.; Santiago, S. M.: Idiopathic Pulmonary Fibrosis: Evaluation with Positron Emission Tomography. *Respiration* **2006**, *73*, 197-202.
[44] Vinson, A. E.; Solis, V.; Williams, H. T.; Bell, B.: F-18-FDG-PET/CT leads to diagnosis of cryptococcal pneumonia where recurrent metastatic rhabdomyosarcoma was suspected. *Clin. Nucl. Med.* **2007**, *32*, 401-3.
[45] Mokhlesi, B.; Angulo-Zereceda, D.; Yaghmai, V.: False-positive FDG-PET scan secondary to lipoid pneumonia mimicking a solid pulmonary nodule. *Ann. Nucl. Med.* **2007**, *21*, 411-4.
[46] Kapucu, L. O.; Meltzer, C. C.; Townsend, D. W.; Keenan, R. J.; Luketich, J. D.: Fluorine-18-fluorodeoxyglucose uptake in pneumonia. *J. Nucl. Med.* **1998**, *39*, 1267-9.
[47] Soussan, M.; Brillet, P. Y.; Mekinian, A.; Khafagy, A.; Nicolas, P.; Vessieres, A.; Brauner, M.: Patterns of pulmonary tuberculosis on FDG-PET/CT. *Eur. J. Radiol.* **2012**, *81*, 2872-6.
[48] Ray, S.; Talukdar, A.; Kundu, S.; Khanra, D.; Sonthalia, N.: Diagnosis and management of miliary tuberculosis: current state and future perspectives. *Ther. Clin. Risk Manag.* **2013**, *9*, 9-26.
[49] Alvarez, J.; Bezos, J.; Juan, L.; Vordermeier, M.; Rodriguez, S.; Fernandez-de-Mera, I. G.; Mateos, A.; Dominguez, L.: Diagnosis of tuberculosis in camelids: old problems, current solutions and future challenges. *Transbound. Emerg. Dis.* **2012**, *59*, 1-10.
[50] Drobniewski, F.; Nikolayevskyy, V.; Balabanova, Y.; Bang, D.; Papaventsis, D.: Diagnosis of tuberculosis and drug resistance: what can new tools bring us? *Int. J. Tuberc. Lung Dis.* **2012**, *16*, 860-70.
[51] Martinez, V.; Castilla-Lievre, M. A.; Guillet-Caruba, C.; Grenier, G.; Fior, R.; Desarnaud, S.; Doucet-Populaire, F.; Boue, F.: (18)F-FDG PET/CT in tuberculosis: an early non-invasive marker of therapeutic response. *Int. J. Tuberc. Lung Dis.* **2012**, *16*, 1180-5.
[52] Sathekge, M.; Maes, A.; Kgomo, M.; Stoltz, A.; Van de Wiele, C.: Use of 18F-FDG PET to Predict Response to First-Line Tuberculostatics in HIV-Associated Tuberculosis. *J. Nucl. Med.* **2011**, *52*, 880-885.
[53] Adkins, A. R.: Establishing a diagnosis of septic arthritis/osteomyelitis - a challenging process. *Equine Vet. Educ.* **2012**, *24*, 615-617.

ISSN 2291-6458 (Print), ISSN 2291-6466 (Online)
Year 2013 | Volume 1 | Issue 2 | Page 85-104

[54] Lankinen, P.; Lehtimaki, K.; Hakanen, A. J.; Roivainen, A.; Aro, H. T.: A comparative 18F-FDG PET/CT imaging of experimental Staphylococcus aureus osteomyelitis and Staphylococcus epidermidis foreign-body-associated infection in the rabbit tibia. *EJNMMI Res.***2012**, *2*, 41.

[55] Kagna, O.; Srour, S.; Melamed, E.; Militianu, D.; Keidar, Z.: FDG PET/CT imaging in the diagnosis of osteomyelitis in the diabetic foot. *Eur. J. Nucl. Med. Mol. Imaging* **2012**, *39*, 1545-50.

[56] Zhuang, H.; Sam, J. W.; Chacko, T. K.; Duarte, P. S.; Hickeson, M.; Feng, Q.; Nakhoda, K. Z.; Guan, L.; Reich, P.; Altimari, S. M.; Alavi, A.: Rapid normalization of osseous FDG uptake following traumatic or surgical fractures. *Eur. J. Nucl. Med. Mol. Imaging* **2003**, *30*, 1096-103.

[57] Guhlmann, A.; Brecht-Krauss, D.; Suger, G.; Glatting, G.; Kotzerke, J.; Kinzl, L.; Reske, S. N.: Chronic osteomyelitis: detection with FDG PET and correlation with histopathologic findings. *Radiology* **1998**, *206*, 749-54.

[58] Ip, D.; Yam, S. K.; Chen, C. K.: Implications of the changing pattern of bacterial infections following total joint replacements. *J. Orthop. Surg. (Hong Kong)* **2005**, *13*, 125-30.

[59] Zhuang, H.; Duarte, P. S.; Pourdehnad, M.; Maes, A.; Van Acker, F.; Shnier, D.; Garino, J. P.; Fitzgerald, R. H.; Alavi, A.: The promising role of 18F-FDG PET in detecting infected lower limb prosthesis implants. *J. Nucl. Med.* **2001**, *42*, 44-8.

[60] Vanquickenborne, B.; Maes, A.; Nuyts, J.; Van Acker, F.; Stuyck, J.; Mulier, M.; Verbruggen, A.; Mortelmans, L.: The value of (18)FDG-PET for the detection of infected hip prosthesis. *Eur. J. Nucl. Med. Mol. Imaging* **2003**, *30*, 705-15.

[61] Love, C.; Marwin, S. E.; Tomas, M. B.; Krauss, E. S.; Tronco, G. G.; Bhargava, K. K.; Nichols, K. J.; Palestro, C. J.: Diagnosing Infection in the Failed Joint Replacement: A Comparison of Coincidence Detection 18F-FDG and 111In-Labeled Leukocyte/99mTc-Sulfur Colloid Marrow Imaging. *J. Nucl. Med.* **2004**, *45*, 1864-1871.

[62] Johnson, J. E.; Kennedy, E. J.; Shereff, M. J.; Patel, N. C.; Collier, B. D.: Prospective study of bone, indium-111-labeled white blood cell, and gallium-67 scanning for the evaluation of osteomyelitis in the diabetic foot. *Foot Ankle Int.* **1996**, *17*, 10-6.

[63] Nawaz, A.; Torigian, D. A.; Siegelman, E. S.; Basu, S.; Chryssikos, T.; Alavi, A.: Diagnostic Performance of FDG-PET, MRI, and Plain Film Radiography (PFR) for the Diagnosis of Osteomyelitis in the Diabetic Foot. *Mol. Imaging Biol.* **2010**, *12*, 335-342.

[64] Hartmann, A.; Eid, K.; Dora, C.; Trentz, O.; von Schulthess, G. K.; Stumpe, K. D.: Diagnostic value of 18F-FDG PET/CT in trauma patients with suspected chronic osteomyelitis. *Eur. J. Nucl. Med. Mol. Imaging* **2007**, *34*, 704-14.

[65] Al-Najjar, A.; Al-Rawahi, G. N.; Hoang, L. M.; Kollmann, T. R.: Clostridium difficile Vertebral Osteomyelitis. *Pediatr. Infect. Dis. J.* **2013**.

[66] Modic, M. T.; Feiglin, D. H.; Piraino, D. W.; Boumphrey, F.; Weinstein, M. A.; Duchesneau, P. M.; Rehm, S.: Vertebral Osteomyelitis - Assessment Using Mr. *Radiology* **1985**, *157*, 157-166.

[67] Gratz, S.; Dorner, J.; Oestmann, J. W.; Opitz, M.; Behr, T. M.; Meller, J.; Becker, W.: Pretreated vertebral osteomyelitis: Evaluation with gallium-67-citrate SPECT. *Eur. J. Nucl. Med.***1999**, *26*, 1004-1004.

[68] Palestro, C. J.; Love, C.; Miller, T. T.: Infection and musculoskeletal conditions: Imaging of musculoskeletal infections. Best *Pract. Res. Clin. Rheumatol.* **2006**, *20*, 1197-218.

[69] Gratz, S.; Dorner, J.; Fischer, U.; Behr, T. M.; Behe, M.; Altenvoerde, G.; Meller, J.; Grabbe, E.; Becker, W.: 18F-FDG hybrid PET in patients with suspected spondylitis. *Eur. J. Nucl. Med. Mol. Imaging* **2002**, *29*, 516-24.

[70] Lopez-Pardo, F.; Gonzalez-Calle, A.; Lopez-Haldon, J.; Acosta-Martinez, J.; Rangel-Sousa, D.; Rodriguez-Puras, M. J.: Real Time Three-Dimensional Transesophageal Echocardiography in the Anatomical Assessment of Complex Mitral Valve Regurgitation Secondary to Endocarditis. *Rev. Esp. Cardiol.* **2012**, *65*, 188-190.

ISSN 2291-6458 (Print), ISSN 2291-6466 (Online)
Year 2013 | Volume 1 | Issue 2 | Page 85-104

[71] Pierce, D.; Calkins, B. C.; Thornton, K.: Infectious Endocarditis: Diagnosis and Treatment. *Am. Fam. Physician* **2012**, *85*, 981-986.
[72] Yen, R. F.; Chen, Y. C.; Wu, Y. W.; Pan, M. H.; Chang, S. C.: Using 18-fluoro-2-deoxyglucose positron emission tomography in detectinq infectious endocarditis/endoarteritis: A preliminary report. *Acad. Radiol.* **2004**, *11*, 316-321.
[73] Cohade, C.: Altered biodistribution on FDG-PET with emphasis on brown fat and insulin effect. *Semin. Nucl. Med.* **2010**, *40*, 283-93.
[74] Balloul, H.: Fever of Undetermined Origin. *Gaz. Med. Fr.* **1989**, *96*, 41-44.
[75] Meller, J.; Becker, W.: Patients with fever of unknown origin (FUO): diagnosis by nuclear medicine imaging. *Nuklearmed* **2001**, *40*, 59-71.
[76] Qiu, L.; Chen, Y.: The role of 18F-FDG PET or PET/CT in the detection of fever of unknown origin. *Eur. J. Radiol.* **2012**, *81*, 3524-9.
[77] Nazar, A. H.; Naswa, N.; Sharma, P.; Soundararajan, R.; Bal, C.; Malhotra, A.; Kumar, R.: Spectrum of 18F-FDG PET/CT findings in patients presenting with fever of unknown origin. *AJR. Am. J. Roentgenol.* **2012**, *199*, 175-85.
[78] Keidar, Z.; Gurman-Balbir, A.; Gaitini, D.; Israel, O.: Fever of unknown origin: the role of 18F-FDG PET/CT. *J. Nucl. Med.* **2008**, *49*, 1980-5.
[79] Goudard, Y.; Pierret, C.; Dusaud, M.; Falzone, E.; Tourtier, J. P.; de Kerangal, X.: Fever of unknown origin: Importance of 18F-FDG PET/CT in the diagnosis of a late infectious complication after aneurysm bypass. *VASA.* **2011**, *40*, 418-21.
[80] Purandare, N. C.; Rangarajan, V.; Shah, S. A.; Sharma, A. R.; Kulkarni, S. S.; Kulkarni, A. V.; Dua, S. G.: Therapeutic Response to Radiofrequency Ablation of Neoplastic Lesions: FDG PET/CT Findings. *Radiographics* **2011**, *31*, 201-U259.
[81] Rehman, T.; Chohan, M.; Yonas, H.: Diagnosis of ventriculoperitoneal shunt infection using [F-18]-FDG PET: a case report. *J. Neurosurg. Sci.* **2011**, *55*, 161-3.
[82] Gotthardt, M.; Bleeker-Rovers, C. P.; Boerman, O. C.; Oyen, W. J. G.: Imaging of Inflammation by PET, Conventional Scintigraphy, and Other Imaging Techniques. *J. Nucl. Med.* **2010**, *51*, 1937-1949.

© 2013 By the Authors; Licensee Borderless Science Publishing, Canada. This is an open access article distributed under the terms and conditions of the Creative Commons Attribution license http://creativecommons.org/licenses/by/3.0/